

Model-free hydrodynamic theory of the colloidal glass transition

Haim Diamant

School of Chemistry and Center for Physics and Chemistry of Living Systems, Tel Aviv University, Tel Aviv 6997801, Israel

(Dated: November 2024)

We present a phenomenological, model-free theory for the large-distance hydrodynamic response of a viscous fluid hosting colloidal particles. The flow of the host fluid is affected by the presence of the particles, thus reflecting their liquid or solid state. On the liquid side of the glass transition we identify a dynamic length scale ℓ beyond which the host fluid's response is that of a viscous fluid with increased effective viscosity η . As the glass transition is approached, ℓ increases indefinitely as $\ell \sim \eta^{1/2}$. At the transition the large-distance response changes qualitatively, marking the host fluid's loss of translation invariance. On the solid side of the transition we identify another dynamic length, ℓ_s , beyond which the host fluid responds as a viscous fluid of increased effective viscosity η^+ , confined in a porous medium of effective pore size ℓ_s . As the glass transition is approached from the solid side, ℓ_s grows indefinitely, more sharply than $(\eta^+)^{1/2}$. We discuss various experimental implications of the results and their possible relation to microscopic theories of the colloidal glass transition.

I. INTRODUCTION

A suspension of colloidal particles in a host fluid solidifies above a certain density or below a certain temperature. The solid may be ordered (a colloidal crystal) or amorphous (a colloidal glass), depending on intricate factors such as small polydispersity of particle size or weak external stresses [1, 2]. Colloidal glasses have been used as convenient model systems to study the elusive glass transition [1–8]. The main advantage over ordinary glasses is that the constituents, the colloidal particles, can be optically visualized and tracked.

It is unclear whether the existence of a host fluid affects the essential features of the glass transition [8–10]. This question is tied to the fundamental issue of whether the mechanism underlying the transition is structural or dynamic [11, 12]. In the present work we turn the spotlight to the host fluid. We investigate changes in its hydrodynamic response to a localized force, caused by the solidification of the suspended particles.

In Sec. II we construct, based on symmetry arguments, an expression for the hydrodynamic response of a generic complex fluid. The response is captured by a set of phenomenological coefficients, one of which serves as an order parameter for the glass transition, i.e., it vanishes in the suspension's liquid state and is nonzero in its solid state. We show that this critical behavior reflects the breaking of translation invariance of the host fluid upon the suspension's solidification. The other coefficients are found to be related to the suspension's global viscosity and to dynamic characteristic length scales. We then use this representation of the host fluid's response to infer properties of the glass transition as it is approached from the liquid side (Sec. III) and the solid side (Sec. IV). In Sec. V we summarize the predictions of the theory, discuss their experimental implications, and suggest possible relations between the results and microscopic theories of the colloidal glass transition. In the Appendix we demonstrate the emergence of the phenomenological coefficients in a simplistic microscopic model.

II. GENERIC HYDRODYNAMIC RESPONSE OF A COMPLEX FLUID

We consider a suspension containing a volume fraction ϕ of particles of typical size a and otherwise arbitrary character, in a fluid of viscosity η_0 . In the absence of particles, the steady flow caused by a force density $\mathbf{f}(\mathbf{r})$ satisfies the following equations [13],

$$-\nabla p + \eta_0 \nabla^2 \mathbf{v} + \mathbf{f}(\mathbf{r}) = 0, \quad (1)$$

$$\nabla \cdot \mathbf{v} = 0, \quad (2)$$

where $\mathbf{v}(\mathbf{r})$ is the local flow velocity and $p(\mathbf{r})$ the local pressure. The Stokes equation (1) arises from the fluid's momentum conservation, $\nabla \cdot \boldsymbol{\sigma} + \mathbf{f} = 0$, where $\sigma_{ij} = -p\delta_{ij} + \eta_0(\partial_i v_j + \partial_j v_i)$ is the momentum flux (stress tensor), and \mathbf{f} the density of momentum sources (force density). Accordingly, Eq. (1) is invariant to the addition of a uniform flow velocity, $\mathbf{v}(\mathbf{r}) \rightarrow \mathbf{v}(\mathbf{r}) + \mathbf{v}_0$, reflecting the fluid's Galilean invariance. Equation (2) accounts for the fluid's mass conservation in the limit of an incompressible fluid.

In Fourier space Eqs. (1) and (2) take the form

$$-i\mathbf{q}p - \eta_0 q^2 \mathbf{v} + \mathbf{f}(\mathbf{q}) = 0, \quad (3)$$

$$\mathbf{q} \cdot \mathbf{v} = 0. \quad (4)$$

Their solution for a point force, $\mathbf{f}(\mathbf{r}) = \mathbf{F}\delta(\mathbf{r}) \rightarrow \mathbf{f}(\mathbf{q}) = \mathbf{F}$, is $\mathbf{v}(\mathbf{q}) = \mathbb{G}^{l,0}(\mathbf{q}) \cdot \mathbf{F}$, where

$$G_{ij}^{l,0}(\mathbf{q}) = \frac{1}{\eta_0 q^2} (\delta_{ij} - \hat{q}_i \hat{q}_j). \quad (5)$$

The pole $q = 0$ in the prefactor reflects momentum conservation as it arises from the conservation equation $i\mathbf{q} \cdot \boldsymbol{\sigma} + \mathbf{f} = 0$. (The pole is double due to the relation between stress and strain rate, $\boldsymbol{\sigma} \sim i\mathbf{q}\mathbf{v}$.) The term in parentheses reflects mass conservation as it ensures the incompressibility condition, $\mathbf{q} \cdot \mathbb{G} = 0$. Inversion of Eq. (5) to real space gives the Oseen tensor [13],

$$G_{ij}^{l,0}(\mathbf{r}) = \frac{1}{8\pi\eta_0 r} (\delta_{ij} + \hat{r}_i \hat{r}_j). \quad (6)$$

If the fluid does not conserve momentum, for example, because of friction with immobile obstacles, Galilean invariance is broken. The simplest way to account for it is to introduce a ‘‘momentum-leaking’’ friction term into the momentum balance equation, $\nabla \cdot \boldsymbol{\sigma} - \Gamma \mathbf{v} + \mathbf{f} = 0$, where Γ is the leakage rate (friction coefficient). For later convenience we rewrite $\Gamma = (\eta_0/a^2)A$ where A is a dimensionless constant. With this addition, Eq. (1) turns into the Brinkman equation [14, 15],

$$-\nabla p + \eta_0[\nabla^2 \mathbf{v} - (A/a^2)\mathbf{v}] + \mathbf{f}(\mathbf{r}) = 0, \quad (7)$$

which is no longer invariant under $\mathbf{v}(\mathbf{r}) \rightarrow \mathbf{v}(\mathbf{r}) + \mathbf{v}_0$. This equation has been widely used to describe viscous flow through porous media. The characteristic length,

$$\xi = aA^{-1/2}, \quad (8)$$

is associated with the typical pore size.

In Fourier space Eq. (7) turns into

$$-i\mathbf{q}p - \eta_0(\xi^{-2} + q^2)\mathbf{v} + \mathbf{f}(\mathbf{q}) = 0. \quad (9)$$

For $\mathbf{f}(\mathbf{r}) = \mathbf{F}\delta(\mathbf{r})$, the solution of this equation together with Eq. (4) is $\mathbf{v}(\mathbf{q}) = \mathbb{G}^{s,0}(\mathbf{q}) \cdot \mathbf{F}$, with

$$G_{ij}^{s,0}(\mathbf{q}) = \frac{1}{\eta_0(\xi^{-2} + q^2)} (\delta_{ij} - \hat{q}_i \hat{q}_j). \quad (10)$$

The $q = 0$ pole in the prefactor has disappeared, indicating the breaking of momentum conservation (i.e., translation invariance). Looking at the first factor only, one expects $\mathbb{G}^s(\mathbf{r})$ in real space to decay exponentially with r/ξ . However, the mass-conservation term still contains a pole in the form $-\hat{q}_i \hat{q}_j = -q_i q_j / q^2$, which transforms to

$$-\frac{q_i q_j}{q^2} \rightarrow \partial_i \partial_j \frac{1}{4\pi r} = -\frac{1}{4\pi r^3} (\delta_{ij} - 3\hat{r}_i \hat{r}_j). \quad (11)$$

Thus, this term gives rise to a long-range $1/r^3$ decay [albeit shorter than the $1/r$ decay of $\mathbb{G}^l(\mathbf{r})$]. It has the angular shape of a dipolar flow as it originates from the effective mass dipole created by the point force over the ‘‘pore’’ size ξ [16, 17]. Full inversion of Eq. (10) gives

$$G_{ij}^{s,0}(\mathbf{r}) = -\frac{1}{4\pi\eta_0\xi} \left\{ \frac{1}{r_s^3} (\delta_{ij} - 3\hat{r}_{s,i} \hat{r}_{s,j}) - \frac{e^{-r_s}}{r_s^3} [(r_s^2 + r_s + 1)\delta_{ij} - (r_s^2 + 3r_s + 3)\hat{r}_{s,i} \hat{r}_{s,j}] \right\}, \quad \mathbf{r}_s = \mathbf{r}/\xi. \quad (12)$$

Over scales larger than the pore size, $r \gg \xi$, the asymptotic response has the expected $1/r^3$ decay, with only exponentially small corrections. For $r \ll \xi$ Eq. (12) reduces to the fluid response, Eq. (6).

The response tensor \mathbb{G} of an isotropic system can conveniently be represented by two scalars, the longitudinal and transverse responses,

$$G_L(r) = G_{xx}(r\hat{\mathbf{x}}), \quad G_T(r) = G_{xx}(r\hat{\mathbf{y}}). \quad (13)$$

Figure 1 shows these response modes for the momentum-conserving fluid [Stokes flow, Eq. (6)] and the momentum-nonconserving one [Brinkman flow, Eq. (12)]. In addition to the different asymptotic decay, $1/r$ and $1/r^3$, respectively,

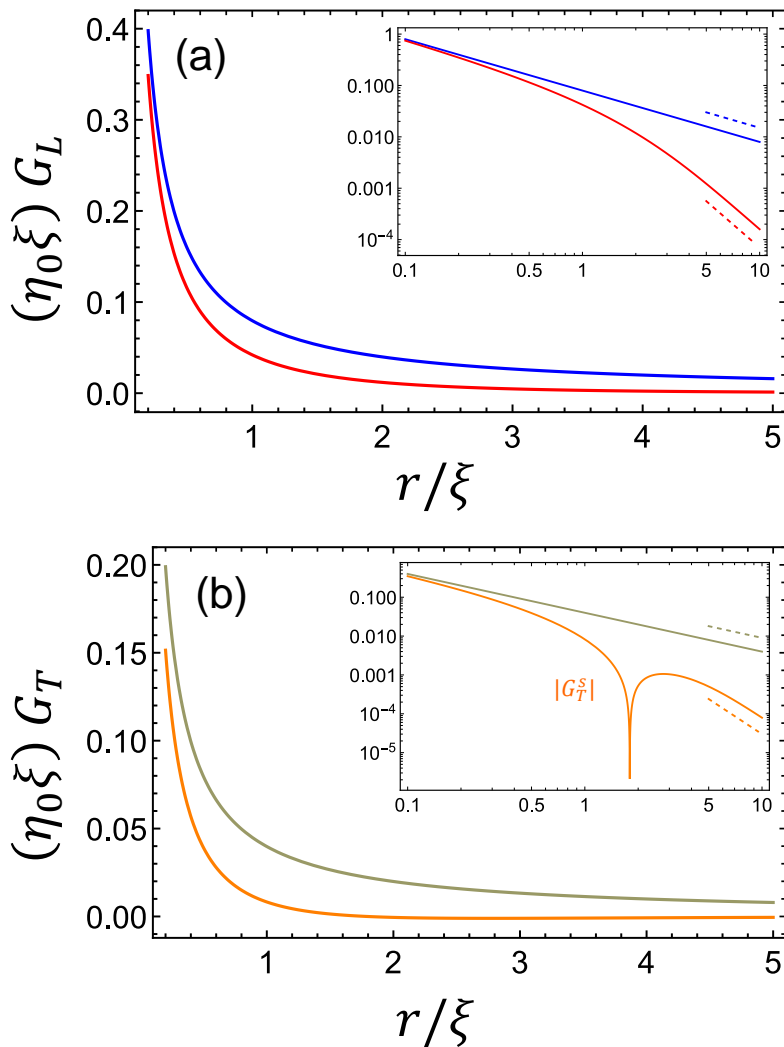


FIG. 1. The longitudinal (a) and transverse (b) hydrodynamic responses as a function of distance from an applied point force, for a momentum-conserving fluid ($G^{l,0}$, upper curves) and a momentum-nonconserving fluid ($G^{s,0}$, lower curves). The insets show the responses on a logarithmic scale, with the dashed lines indicating $1/r$ and $1/r^3$ decays. The responses are scaled by $(\eta_0 \xi)^{-1}$ and the distance by ξ . For $r \ll \xi$, $G_{L,T}^{l,0}$ and $G_{L,T}^{s,0}$ coincide. The transverse response $G_T^{s,0}$ becomes negative for $r/\xi \gtrsim 1$ [panel (b) inset].

the momentum-nonconserving fluid has another distinctive feature. Its asymptotic transverse response is negative. This follows from the dipolar shape of the first term in Eq. (12), as mentioned above.

As concerns complex fluids, such as colloidal suspensions and polymer networks, the two hydrodynamic responses discussed above correspond to two limits where the flow is of the host fluid alone. Equations (5) and (6) give the response of the particle-free fluid, i.e., the limit of vanishing volume fraction of particles. Equations (10) and (12) give the response in the case where the host fluid flows past an immobile matrix. As these two extremes are separated by a symmetry breaking, their asymptotic spatial decays are distinct. The translational symmetry breaking is captured by the coefficient A , which serves as an order parameter, becoming nonzero when the symmetry is broken. Moreover, the asymptotic $1/r$ and $1/r^3$ power laws arise from conservation laws of momentum and mass, respectively. Hence, they must hold for the host fluid's response in any liquid and solid suspension, respectively [16, 17].

In the present work we would like to treat suspensions away from these two limits, in particular, in the vicinity of the symmetry breaking. As the volume fraction ϕ of a suspension is increased from zero, length scales emerge which characterize the structure of the suspended particles. A natural way to introduce these length scales into the coarse-grained hydrodynamic response by the following extension of Eqs. (3) and (9),

$$-i\mathbf{q}p + \eta_0[-A/a^2 + B(iq)^2 + Ca^2(iq)^4 + Da^4(iq)^6 + \dots]\mathbf{v} + \mathbf{f}(\mathbf{q}) = 0. \quad (14)$$

where $A(\phi), B(\phi), C(\phi), D(\phi), \dots$ are dimensionless coefficients which depend on the volume fraction (and in general also the temperature).¹ Each additional term accounts for the effect of a higher-order velocity gradient, i.e., a smaller (yet still large compared to a) length scale.² The solution of Eq. (14) for a point force $\mathbf{f}(\mathbf{r}) = \mathbf{F}\delta(\mathbf{r})$, together with the incompressibility condition (4), is $\mathbf{v} = \mathbb{G} \cdot \mathbf{F}$ with

$$G_{ij}(\mathbf{q}) = \frac{1}{\eta_0(A/a^2 + Bq^2 - Ca^2q^4 + Da^4q^6 - \dots)} (\delta_{ij} - \hat{q}_i\hat{q}_j). \quad (15)$$

The Ansatz in Eq. (15) concerning the hydrodynamic response of the host fluid is our starting point, from which the rest of the results inevitably follow. The generic expansion in Eqs. (14) and (15) assumes only that the host fluid remains rotation- and inversion-symmetric, and incompressible, thus making the theory model-free. The details of a specific system are absorbed in the unspecified dependencies of the phenomenological coefficients A, B, C, D, \dots on ϕ (and temperature).¹ In the Appendix we obtain the leading coefficients explicitly for a simplistic example.

III. LIQUID SIDE OF THE TRANSITION

In a liquid suspension, where all constituents are mobile and momentum is conserved, $A = 0$ exactly. We rewrite Eq. (15) as

$$G_{ij}(\mathbf{q}) = \frac{1}{\eta_0 B[q^2 - (C/B)a^2q^4 + (D/B)a^4q^6 - \dots]} (\delta_{ij} - \hat{q}_i\hat{q}_j), \quad (16)$$

which can be decomposed as

$$G_{ij}^l(\mathbf{q}) = \left[\frac{1}{\eta q^2} + \frac{1 - (D/C)a^2q^2 + \dots}{\eta(\ell^{-2} - q^2 + (D/C)a^2q^4 - \dots)} \right] (\delta_{ij} - \hat{q}_i\hat{q}_j), \quad (17)$$

$$\eta(\phi) = \eta_0 B(\phi), \quad (18)$$

$$\ell(\phi) = a[C(\phi)/B(\phi)]^{1/2}. \quad (19)$$

The first term in Eq. (17) coincides with the response of a momentum-conserving fluid, Eq. (5), except that the particle-free viscosity η_0 has been replaced by $\eta(\phi) = B(\phi)\eta_0$. Thus the coefficient $B(\phi)$ relates to the effective viscosity of the suspension. The second term in Eq. (17) contains a pole structure that depends on the roots of the polynomial $(\ell^{-2} - q^2 + (D/C)a^2q^4 - \dots)$. Each of these roots will give rise in real space to an exponential term with a certain decay length (and possibly also oscillation wavelength if the root is complex), reflecting the structure of the suspension. However, for any finite ℓ , the polynomial does not have a root equal to zero. The only $q = 0$ root comes, as in the response of a momentum-nonconserving fluid [Eq. (10)], from the dipolar mass term, $-(\ell^2/\eta)q_iq_j/q^2$. Therefore, we can directly read from Eqs. (6) and (12) the large-distance response of the liquid suspension as

$$G_{ij}^l(\mathbf{r}) = \frac{1}{8\pi\eta r} (\delta_{ij} + \hat{r}_i\hat{r}_j) - \frac{\ell^2}{4\pi\eta r^3} (\delta_{ij} - 3\hat{r}_i\hat{r}_j), \quad (20)$$

with exponentially small corrections.

Thus the host fluid's response contains a solid-like component as a subdominant term at large distances. It arises from the effective mass dipole created by the point force over the intrinsic length scale $\ell(\phi)$, similar to the one formed in a momentum-nonconserving fluid over the length scale ξ (where this term is dominant). The distance $r \sim \ell$ marks a crossover from the liquid-like response, $\sim 1/(\eta r)$, for $r \gtrsim \ell$, to the solid-like one, $\sim \ell^2/(\eta r^3)$, for $r \lesssim \ell$. The longitudinal and transverse responses arising from Eq. (20) are plotted in Fig. 2.

As the glass transition is approached, $\eta(\phi)$ grows indefinitely, making the dominant response, $\sim 1/(\eta r)$ increasingly weak. As we have seen in Sec. II, however, the momentum-nonconserving response of the host fluid is finite in a solid. Hence, the subdominant term, $\sim \ell^2/\eta$, should remain finite. This implies that the crossover length $\ell(\phi)$ must grow indefinitely as well, as³

$$\ell(\phi) \sim \eta(\phi)^{1/2} \xrightarrow{\eta \rightarrow \infty} \infty. \quad (21)$$

¹ In this work we address the suspension's purely viscous response, i.e., the limit of vanishing frequency. More generally, for a viscoelastic suspension or gel, these coefficients will be frequency-dependent.

² An equivalent way to view Eq. (14) is to consider the entire factor multiplying \mathbf{v} as a q -dependent (and possibly also frequency-dependent) viscosity [18].

³ If the suspension has no other intrinsic structural length than a , and no other intrinsic time than $a^2/(\eta_0/\rho_0)$ (ρ_0 being the mass density of the host fluid), then, on dimensional grounds, $\ell(\phi) \sim (a/\eta_0)\eta(\phi)$. Equivalently, $\ell^2/\eta \sim a^2/\eta_0$. The physical interpretation is that the strength of the mass dipole, underlying the $1/r^3$ response, depends on the local viscosity rather than the suspension's large-scale viscosity $\eta(\phi)$.

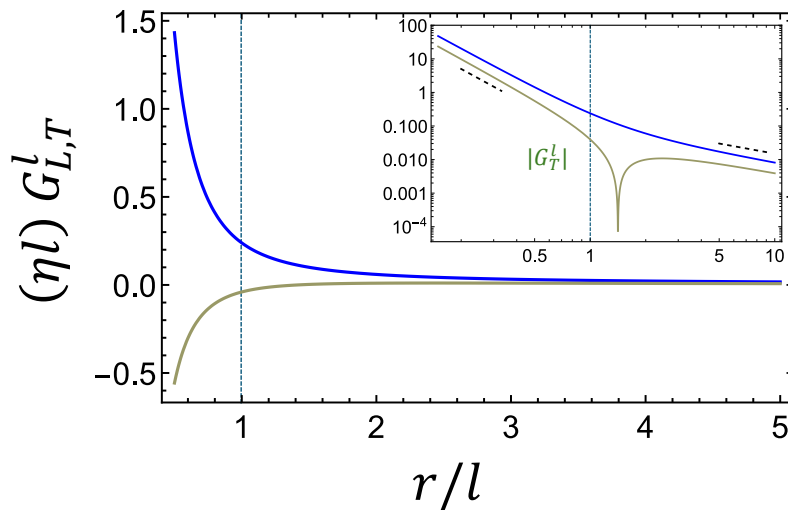


FIG. 2. The longitudinal (upper curve) and transverse (lower curve) hydrodynamic responses as a function of distance from an applied point force, for a liquid suspension. The inset shows the responses on a logarithmic scale, with the dashed lines indicating $1/r$ and $1/r^3$ decays. The responses are scaled by $(\eta\ell)^{-1}$ and the distance by ℓ . Below the distance $r \sim \ell$ (dotted vertical lines) the response crosses over from a $1/r$ decay to a $1/r^3$ decay, and the transverse response becomes negative.

IV. SOLID SIDE OF THE TRANSITION

For a solid we have $A > 0$, leading to a qualitatively different response at large distances. We return to Eq. (15) and rewrite it now as

$$G_{ij}^s(\mathbf{q}) = \frac{1}{\eta^+[\ell_s^{-2} + q^2 - (C^+/B^+)a^2q^4 + (D^+/B^+)a^4q^6 - \dots]} (\delta_{ij} - \hat{q}_i\hat{q}_j). \quad (22)$$

$$\eta^+(\phi) = \eta_0 B^+(\phi), \quad (23)$$

$$\ell_s(\phi) = a[B^+(\phi)/A(\phi)]^{1/2} = \xi[\eta^+(\phi)/\eta_0]^{1/2}. \quad (24)$$

We have added the superscript ‘+’ to indicate that the coefficients B, C, D, \dots are not supposed to have the same ϕ -dependence below and above the transition. As before, the detailed response depends on the pole structure of Eq. (22), but, for any finite ℓ_s , the only $q = 0$ pole comes again from the mass-dipole term, $-(\ell_s^2/\eta^+)q_i q_j/q^2$. Hence, replacing η_0 by η^+ and ξ by ℓ_s , we can directly read from Eq. (12) the large-distance response of the host fluid in the solid suspension,

$$G_{ij}^s(\mathbf{r}) = -\frac{\ell_s^2}{4\pi\eta^+r^3} (\delta_{ij} - 3\hat{r}_i\hat{r}_j), \quad r > \ell_s, \quad (25)$$

with corrections that are exponentially small in r/ℓ_s . The longitudinal and transverse components of this response are shown in Fig. 3. For $r \gtrsim \ell_s$ [the domain where Eq. (25) is valid], the transverse correlation is negative.

Thus the host fluid in a solid suspension behaves over large scales like a Brinkman fluid with effective viscosity $\eta^+(\phi)$ and effective pore size $\ell_s(\phi)$. Away from the glass transition the solid matrix should become rigid, and we expect B^+ to tend to 1, making η^+ tend to η_0 and ℓ_s tend to ξ , thus coinciding with the Brinkman parameters for a rigid porous medium [Eqs. (10) and (12)]. As the glass transition is approached from the solid side, assuming that amorphous solidification is a continuous transition, $A(\phi)$ should continuously decrease to zero. This is accompanied by changes of η^+ and ℓ_s . According to Eqs. (23) and (24), ℓ_s must diverge at least as sharply as $A^{-1/2}$. In addition, just above the transition, there is a single effective pore of size $\ell_s \rightarrow \infty$, whose viscosity η^+ must diverge as well to describe a solid. Hence, ℓ_s increases close to the transition more sharply than $A^{-1/2}$,

$$\ell_s(\phi) \sim A(\phi)^{-1/2} \eta^+(\phi)^{1/2} \xrightarrow{A \rightarrow 0, \eta^+ \rightarrow \infty} \infty. \quad (26)$$

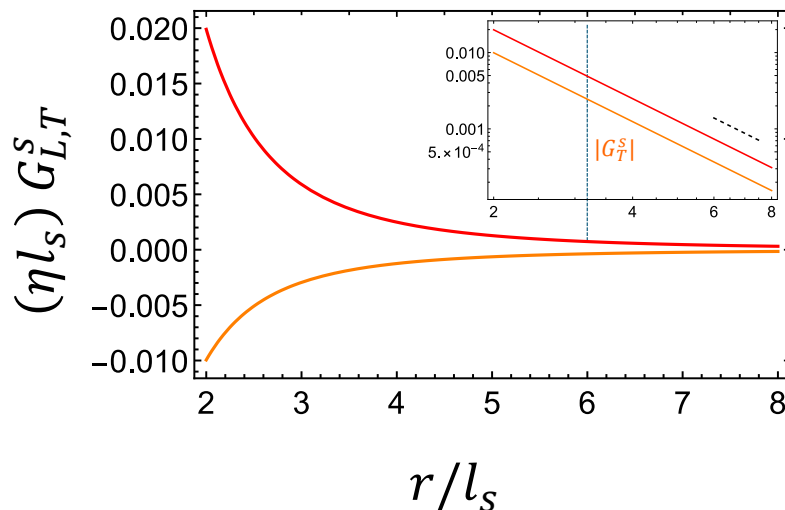


FIG. 3. The longitudinal (upper curve) and transverse (lower curve) hydrodynamic responses as a function of distance from an applied point force, at large distances, for a solid suspension. The inset shows the responses on a logarithmic scale, with the dashed line indicating a $1/r^3$ decay. The responses are scaled by $(\eta^+ \ell_s)^{-1}$ and the distance by ℓ_s . For $r \gtrsim \ell_s$ the transverse response is negative.

V. DISCUSSION

We have introduced a set of phenomenological coefficients, characterizing the hydrodynamic response of a suspension’s host fluid over decreasing (yet large) distances, and demanded that the fluid’s conservation laws be satisfied or broken. This has led to a set of nontrivial conclusions. We begin by summarizing the predictions of the theory.⁴

The solidification of the suspended particles causes a critical behavior of their host fluid. The critical behavior is captured by three phenomenological coefficients, $A(\phi)$, $B(\phi)$, and $C(\phi)$, which should depend also on temperature and be different on the two sides of the transition. The coefficient A serves as an order parameter, being strictly zero in a liquid suspension, where the host fluid is translation-invariant, and nonzero in a solid suspension, where the translation invariance of the host fluid is broken. The coefficient B is the ratio between the effective viscosity η and the viscosity η_0 of the pristine host fluid.

Below the glass transition ($A = 0$) B and C give rise to a dynamic length $\ell \sim (C/B)^{1/2}$. It marks the crossover of the host fluid’s response from a $1/(\eta r)$ decay at asymptotically large distances to a “solid-like” $\ell^2/(\eta r^3)$ decay at smaller distances. The latter’s transverse component is negative. The dynamic length ℓ increases with effective viscosity as $\ell \sim \eta^{1/2}$ [19]. Thus, as η increases, the crossover occurs at an increasingly large distance, until, at the transition, the solid-like $1/r^3$ response takes over the whole system. If the effective viscosity (or the relaxation time) diverges as a power law [3],

$$\eta(\phi) \sim (\phi_c - \phi)^{-\zeta} \quad \phi \nearrow \phi_c, \quad (27)$$

with some exponent ζ , then

$$\ell(\phi) \sim (\phi_c - \phi)^{-\zeta/2}, \quad \phi \nearrow \phi_c^-. \quad (28)$$

We would like to underline the significance and usefulness of the transverse response’s different sig for $r \lesssim \ell$ and $r \gtrsim \ell$. As long as the transverse response approaches zero from above at very large distances, the suspension is overall liquid. This is a clearcut experimental criterion which does not require fitting. Unlike the common tests of glassiness, such as the confined dynamics of single particles or a non-decaying dynamic scattering function at $q \sim 1/a$, this test offers a probe of the suspension’s *large-scale* fluidity or solidity.

Above the transition ($A > 0$) the coefficients A and B give rise to a dynamic length $\ell_s \sim (B/A)^{1/2}$. It acts as a dynamic “pore” size beyond which the solid matrix affects the host fluid as a stationary porous medium. Assuming

⁴ We refer here to the transition point in terms of a critical volume fraction ϕ_c for a fixed temperature. We may just as well consider a critical temperature at a fixed volume fraction (for thermal systems, i.e., not merely hard spheres).

that the transition is continuous, one expects the symmetry breaking to affect the order parameter as

$$A(\phi) \sim (\phi - \phi_c)^\beta, \quad \phi \searrow \phi_c, \quad (29)$$

with some exponent β . If, in addition, the effective pore viscosity increases as

$$\eta^+(\phi) \sim (\phi - \phi_c)^{-\zeta^+}, \quad \phi \searrow \phi_c, \quad (30)$$

then the dynamic length on the solid size diverges as

$$\ell_s(\phi) \sim (\phi - \phi_c)^{-(\beta+\zeta^+)/2}, \quad \phi \searrow \phi_c. \quad (31)$$

Most of the predictions concerning the approach to the glass transition from the liquid side have been verified in recent experiments by Egelhaaf and coworkers [20]: (a) the asymptotic $1/(\eta r)$ response with $\eta(\phi)$ as the suspension's effective viscosity; (b) the crossover to the $\ell^2/(\eta r^3)$ response at smaller distances, with a negative transverse component; (c) the sharply increasing length $\ell(\phi)$, extracted from the crossover, as the transition is approached. The experiments used confocal microscopy to track the correlated Brownian motions of pairs of tracer particles in a suspension of much larger particles. The measured displacement correlations of the tracers are proportional to the responses calculated here owing to the fluctuation-dissipation theorem [21]. The experiments were not able to check the predictions concerning the solid suspension. For all the studied volume fractions the suspension was found to be a liquid [22] over large distances, using the transverse-response criterion mentioned above.

The results of the present work have been obtained from the phenomenological Ansatz of Eq. (15) and do not depend on a specific microscopic (particle-based) model. This has pros and cons. One advantage is that the predictions should apply to any complex fluid containing a molecular host fluid. Indeed, the crossover from the asymptotic $1/r$ response to the $1/r^3$ one, with the associated crossover length ℓ , were observed not only in colloidal suspensions [20] but also in entangled networks of semiflexible polymers [23, 24]. Thus our findings should be relevant for transitions in other complex fluids such as fiber networks [25] and the cytoplasm [26]. Another advantage is that the results follow from a minimum set of assumptions and can be used to test the validity of more detailed theories.

This work's obvious shortcoming is the lack of information concerning the particle-level mechanisms behind the transition. Microscopic models (e.g., for hard sphere) should be able to provide explicit expressions for the coefficients A, B, C, D, \dots . Nevertheless, the phenomenological description of the transition obtained here suggests a relation to observations concerning dynamic heterogeneities [11]. On the liquid side, the solid-resembling dynamic response for $r \lesssim \ell$ may be associated with clusters [8, 27] of typical size ℓ in an overall liquid suspension. On the solid side, the growing effective ‘‘pores’’ of typical size ℓ_s may be associated with liquid ‘‘soft spots’’ in an overall solid suspension [28]. In addition, the order parameter $A(\phi)$ might be interpreted in terms of the fraction of immobile particles (see the Appendix).

In conclusion, the phenomenological theory developed above reveals symmetry-related constraints imposed on the host fluid below and above the colloidal glass transition. It highlights the transition's critical effect on the dynamics of the host fluid and what can be learned from this effect on the transition. The theory thus sets colloidal glasses apart from molecular glasses. The predictions concerning the solid side of the transition are yet to be checked experimentally. The correspondence between the hydrodynamic theory and particle-based theories calls for further investigation.

ACKNOWLEDGMENTS

The theory was developed to accompany experiments by Prof. Dr. Stefan U. Egelhaaf and his group [20]. This article is dedicated to the dear memory of Stefan. I am grateful to Patrick Laermann, Manuel Escobedo-Sánchez, Yael Roichman, and Ivo Buttinoni, who participated in that joint project. I thank Paddy Royall for illuminating talks. The research was supported by the German-Israeli Foundation (GIF Grant no. I-1345-303.10-2016) and the Israel Science Foundation (ISF Grant no. 1611/24).

Appendix: Particle-based model

This Appendix demonstrates the emergence of the phenomenological coefficients introduced in Sec. II in a specific, simplistic example. The model consists of hard spheres of radius a and number density c suspended in a viscous host fluid of viscosity η_0 . A fraction α of the particles are restricted in their motion to the vicinity of a certain position, whereas the rest, a fraction of $1 - \alpha$, are free to move. As regards the hydrodynamics of the host fluid, the former

particles can resist a force whereas the latter particles are force- and torque-free. For simplicity we assume that the restricted particles are torque-free. The extension to particles whose rotation is restricted as well is straightforward. Our aim is to calculate the large-distance hydrodynamic response of the host fluid to leading order in c . Practically, it is inconsistent to assume that particles are spontaneously restricted (caged) in a dilute suspension. This, and the neglect of positional correlations, limits the model to demonstrative purposes. Still, one can come up with physical scenarios where the situation described above is achievable, e.g., by applying optical traps to immobilize a fraction of particles in a dilute suspension.

We consider a point force, $\mathbf{F}\delta(\mathbf{r})$, applied to the host fluid at the origin. To zeroth order in c , the force creates the flow velocity [see Eq. (6)]

$$\mathbf{v}^0(\mathbf{r}) = \mathbb{G}^0(\mathbf{r}) \cdot \mathbf{F}, \quad G_{ij}^0(\mathbf{r}) = \frac{1}{8\pi\eta_0 r} (\delta_{ij} + \hat{r}_i \hat{r}_j). \quad (\text{A.1})$$

Next we consider a particle located at \mathbf{r}' and experiencing the flow (A.1). A restricted particle responds by exerting a force given by Faxén's first law [13],

$$\mathbf{F}^1(\mathbf{r}') = -6\pi\eta_0 a [1 + (a^2/6)\nabla^2] \mathbf{v}^0(\mathbf{r}') = -6\pi\eta_0 a [1 + (a^2/6)\nabla^2] \mathbb{G}^0(\mathbf{r}') \cdot \mathbf{F}, \quad (\text{A.2})$$

and a symmetric force dipole (stresslet) given by Faxén's third law [13],

$$\begin{aligned} \mathbb{S}^1(\mathbf{r}') &= \frac{10\pi}{3} \eta_0 a^3 [1 + (a^2/10)\nabla^2] [\nabla \mathbf{v}^0(\mathbf{r}') + (\nabla \mathbf{v}^0(\mathbf{r}'))^T] \\ &= \frac{10\pi}{3} \eta_0 a^3 [1 + (a^2/10)\nabla^2] [\nabla \mathbb{G}^0(\mathbf{r}') \cdot \mathbf{F} + (\nabla \mathbb{G}^0(\mathbf{r}'))^T \cdot \mathbf{F}], \end{aligned} \quad (\text{A.3})$$

assuming that it is torque-free. A force- and torque-free particle responds by \mathbb{S}^1 alone. For a rigid sphere there are no higher force moments [13]. The force introduced by a restricted particle at \mathbf{r}' changes the flow at \mathbf{r} by

$$\mathbf{v}_F^1(\mathbf{r}, \mathbf{r}') = \mathbb{G}^0(\mathbf{r} - \mathbf{r}') \cdot \mathbf{F}^1(\mathbf{r}'). \quad (\text{A.4})$$

The force dipole introduced by either type of particle at \mathbf{r}' changes the flow at \mathbf{r} by

$$\mathbf{v}_S^1(\mathbf{r}, \mathbf{r}') = \nabla \mathbb{G}^0(\mathbf{r} - \mathbf{r}') \cdot \mathbb{S}^1(\mathbf{r}'). \quad (\text{A.5})$$

We now add the contributions to the flow at \mathbf{r} from all the particles. To linear order in c the probability densities of finding a restricted or free particle at a certain position are uniform and equal to αc and $(1 - \alpha)c$, respectively. Thus the average flow velocity at \mathbf{r} is given by

$$\langle \mathbf{v}(\mathbf{r}) \rangle = \mathbf{v}^0(\mathbf{r}) + c \int d\mathbf{r}' [\alpha \mathbf{v}_F^1(\mathbf{r}, \mathbf{r}') + \mathbf{v}_S^1(\mathbf{r}, \mathbf{r}')]. \quad (\text{A.6})$$

Transforming Eqs. (A.2)–(A.6) to Fourier space, with

$$G_{ij}^0(\mathbf{q}) = \frac{1}{\eta_0 q^2} (\delta_{ij} - \hat{q}_i \hat{q}_j), \quad (\text{A.7})$$

and making use of the convolution theorem, we find

$$\begin{aligned} \langle \mathbf{v}(\mathbf{q}) \rangle &= \mathbb{G}(\mathbf{q}) \cdot \mathbf{F} \\ \mathbb{G}(\mathbf{q}) &= \mathbb{G}^0(\mathbf{q}) - \frac{\pi a c}{q^2} [6\alpha + (10/3 - \alpha)a^2 q^2 - (1/3)a^4 q^4] \mathbb{G}^0(\mathbf{q}). \end{aligned} \quad (\text{A.8})$$

This can be rearranged, to leading order in c , as

$$G_{ij}(\mathbf{q}) = \frac{1}{\eta_0} \frac{1}{(9/2)\alpha\phi/a^2 + [1 + (5/2)\phi(1 - 3\alpha/10)]q^2 - (\phi a^2/4)q^4} (\delta_{ij} - \hat{q}_i \hat{q}_j). \quad (\text{A.9})$$

where we have replaced $\phi = (4\pi a^3/3)c$. Comparing with Eq. (15) we read

$$A = \frac{9}{2}\alpha\phi, \quad B = 1 + \frac{5}{2}\phi \left(1 - \frac{3}{10}\alpha\right), \quad C = \frac{1}{4}\phi. \quad (\text{A.10})$$

Thus the order parameter A is proportional to the fraction α of restricted particles, i.e., as expected, it vanishes for a liquid suspension where all particles are free. The effective viscosity $\eta = \eta_0 B$ is appropriately positive. For $\alpha = 0$ it coincides with the classical result [29], $\eta = \eta_0[1 + (5/2)\phi]$. For $\alpha > 0$ it decreases with α , which may seem non-intuitive but is the appropriate trend. As discussed in Sec. IV, when we get further away from the transition on the solid side, the effective pore size $\ell_s \sim (B/A)^{1/2}$ decreases toward ξ and its effective viscosity decreases toward η_0 . Because of the dependence on $\alpha(\phi)$, B has a different ϕ -dependence on the two sides of the transition.

-
- [1] P. N. Pusey and W. van Meegen, Phase behaviour of concentrated suspensions of nearly hard colloidal spheres, *Nature* **320**, 340 (1986).
- [2] Z. Cheng, P. M. Chaikin, W. B. Russel, W. V. Meyer, J. Zhu, R. B. Rogers, and R. H. Ottewill, Phase diagram of hard spheres, *Mater. Design* **22**, 529 (2001).
- [3] L. Cipelletti and E. R. Weeks, in *Dynamical Heterogeneities in Glasses, Colloids, and Granular Media*, L. Berthier, G. Biroli, J.-P. Bouchaud, L. Cipelletti, and W. van Saarloos, Eds., (Oxford University Press, 2011).
- [4] G. L. Hunter and E. R. Weeks, The physics of the colloidal glass transition, *Rep. Prog. Phys.* **75**, 066501 (2012).
- [5] S. Gokhale, A. K. Sood, and R. Ganapathy, Deconstructing the glass transition through critical experiments on colloids, *Adv. Phys.* **65**, 363 (2016).
- [6] O. Dauchot, F. Ladieu, C. P. Royall, The glass transition in molecules, colloids and grains: universality and specificity, *Compt. Rend. Phys.* **24**, 25 (2023).
- [7] E. R. Weeks, J. C. Crocker, A. C. Levitt, A. Schoefield A, and D. A. Weitz, Three-dimensional direct imaging of structural relaxation near the colloidal glass transition, *Science* **287**, 627 (2000).
- [8] J. C. Conrad, P. P. Dhillon, E. R. Weeks, D. R. Reichman, and D. A. Weitz, Contribution of slow clusters to the bulk elasticity near the colloidal glass transition, *Phys. Rev. Lett.* **97**, 265701 (2006).
- [9] A. Furukawa and H. Tanaka, Key role of hydrodynamic interactions in colloidal gelation, *Phys. Rev. Lett.* **104**, 245702 (2010).
- [10] M. Tateno, T. Yanagishima, J. Russo, and H. Tanaka, Influence of hydrodynamic interactions on colloidal crystallization, *Phys. Rev. Lett.* **123**, 258002 (2019).
- [11] L. Berthier, G. Biroli, J.-P. Bouchaud, L. Cipelletti, and W. van Saarloos, Eds., *Dynamical Heterogeneities in Glasses, Colloids, and Granular Media* (Oxford University Press, 2011).
- [12] P. G. Wolynes and V. Lubchenko, Eds., *Structural Glasses and Supercooled Liquids: Theory, Experiment, and Applications* (Wiley, 2012).
- [13] J. Happel and H. Brenner, *Low Reynolds Number Hydrodynamics with Special Applications to Particulate Media*, 3rd Ed. (Springer, 1983).
- [14] H. C. Brinkman, A calculation of the viscous force exerted by a flowing fluid on a dense swarm of particles, *Appl. Sci. Res.* **A1**, 27 (1949).
- [15] L. Durlofsky and J. F. Brady, Analysis of the Brinkman equation as a model for flow in porous media, *Phys. Fluids* **30**, 3329 (1987).
- [16] H. Diamant, Long-range hydrodynamic response of particulate liquids and liquid-laden solids, *Israel J. Chem.* **47**, 225 (2007).
- [17] H. Diamant, Hydrodynamic interaction in confined geometries, *J. Phys. Soc. Jpn.* **78**, 041002 (2009).
- [18] A. Y. Grosberg, J.-F. Joanny, W. Srinin, and Y. Rabin, Scale-dependent viscosity in polymer fluids, *J. Phys. Chem. B* **120**, 6383 (2016).
- [19] J. Hu, L. Ning, R. Liu, M. Yang, K. Chen, Evidence for growing structural correlation length in colloidal supercooled liquids, *Phys. Rev. E* **106**, 054601 (2022).
- [20] P. Laermann, H. Diamant, Y. Roichman, I. Buttinoni, M. A. Escobedo-Sánchez, and S. U. Egelhaaf, New signatures of the glass transition in colloidal suspensions, submitted for publication.
- [21] J. C. Crocker, M. T. Valentine, E. R. Weeks, T. Gisler, P. D. Kaplan, A. G. Yodh, and D. A. Weitz, Two-point microrheology of inhomogeneous soft materials, *Phys. Rev. Lett.* **85**, 888 (2000).
- [22] G. Brambilla, D. El Masri, M. Pierno, L. Berthier, L. Cipelletti, G. Petekidis, and A. B. Schofield, Probing the equilibrium dynamics of colloidal hard spheres above the mode-coupling glass transition, *Phys. Rev. Lett.* **102**, 085703 (2009).
- [23] A. Sonn-Segev, A. Bernheim-Groswasser, H. Diamant, and Y. Roichman, Viscoelastic response of a complex fluid at intermediate distances, *Phys. Rev. Lett.* **112**, 088301 (2014).
- [24] A. Sonn-Segev, A. Bernheim-Groswasser, and Y. Roichman, Extracting the dynamic correlation length of actin networks from microrheology experiments, *Soft Matter* **10**, 8324 (2014).
- [25] A. J. Licup, S. Münster, A. Sharma, M. Sheinman, L. M. Jawerth, B. Fabry, D. A. Weitz, and F. C. MacKintosh, Stress controls the mechanics of collagen networks, *Proc. Natl. Acad. Sci. USA* **112**, 9573 (2015).
- [26] E. H. Zhou, X. Trepas, C. Y. Park, G. Lenormand, M. N. Oliver, S. M. Mijailovich, C. Hardin, D. A. Weitz, J. P. Butler, and J. J. Fredberg, Universal behavior of the osmotically compressed cell and its analogy to the colloidal glass transition, *Proc. Natl. Acad. Sci. USA* **106**, 10632 (2009).
- [27] K. Kroy, M. E. Cates, and W. C. K. Poon, Cluster mode-coupling approach to weak gelation in attractive colloids, *Phys. Rev. Lett.* **92**, 148302 (2004).

- [28] E. Aharonov, E. Bouchbinder, H. G. E. Hentschel, V. Ilyin, N. Makedonska, I. Procaccia, and N. Schupper, Direct identification of the glass transition: Growing length scale and the onset of plasticity, *Europhys. Lett.* **77**, 56002 (2007).
- [29] A. Einstein, *Investigations on the Theory of the Brownian Movement* (Dover, 1954).